

Catalytic Mechanism of Dopamine β -Monooxygenase Mediated by Cu(III)–Oxo

Kazunari Yoshizawa,* Naoki Kihara, Takashi Kamachi, and Yoshihito Shiota

Institute for Materials Chemistry and Engineering, Kyushu University, Fukuoka 812-8581, Japan

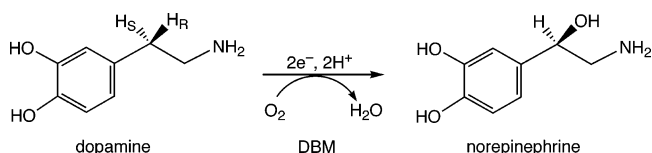
Received December 11, 2005

Mechanisms of dopamine hydroxylation by the Cu(II)–superoxo species and the Cu(III)–oxo species of dopamine β -monooxygenase (DBM) are discussed using QM/MM calculations for a whole-enzyme model of 4700 atoms. A calculated activation barrier for the hydrogen-atom abstraction by the Cu(II)–superoxo species is 23.1 kcal/mol, while that of the Cu(III)–oxo, which can be viewed as Cu(II)–O \cdot , is 5.4 kcal/mol. Energies of the optimized radical intermediate in the superoxo- and oxo-mediated pathways are 18.4 and –14.2 kcal/mol, relative to the corresponding reactant complexes, respectively. These results demonstrate that the Cu(III)–oxo species can better mediate dopamine hydroxylation in the protein environment of DBM. The side chains of three amino acid residues (His415, His417, and Met490) coordinate to the Cu_B atom, one of the copper sites in the catalytic core that plays a role for the catalytic function. The hydrogen-bonding network between dopamine and the three amino acid residues (Glu268, Glu369, and Tyr494) plays an essential role in substrate binding and the stereospecific hydroxylation of dopamine to norepinephrine. The dopamine hydroxylation by the Cu(III)–oxo species is a downhill and lower-barrier process toward the product direction with the aid of the protein environment of DBM. This enzyme is likely to use the high reactivity of the Cu(III)–oxo species to activate the benzylic C–H bond of dopamine; the enzymatic reaction can be explained by the so-called oxygen rebound mechanism.

1. Introduction

Dopamine β -monooxygenase (DBM; EC 1.14.17.1) catalyzes the transformation of dopamine and dioxygen into norepinephrine and water, as shown in Scheme 1.^{1–8} These two molecules are important neurotransmitters; dopamine depresses blood pressure, while norepinephrine raises blood pressure.^{9,10} Battersby et al.¹¹ demonstrated from the analysis of deuterium and tritium isotope effects that the pro-R

Scheme 1



hydrogen atom of the benzylic position of dopamine is stereospecifically abstracted in the course of this enzymatic process.

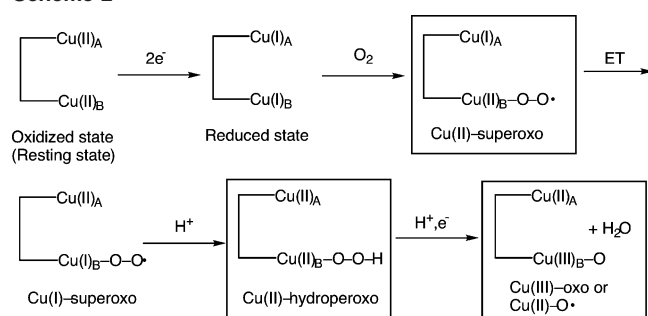
DBM contains two copper atoms per subunit.^{12–14} They are at least 4 Å apart because no spin coupling is detected by electron spin resonance (ESR) measurements in the resting enzyme and the product complex.^{15,16} EXAFS experiments¹⁷

* To whom correspondence should be addressed. E-mail: kazunari@ms.ifoc.kyushu-u.ac.jp.

- (1) Levin, E. Y.; Levenberg, B.; Kaufman, S. *J. Biol. Chem.* **1960**, *235*, 2080.
- (2) Skotland, T.; Ljones, T. *Inorg. Perspect. Biol. Med.* **1979**, *2*, 151.
- (3) Rosenberg, R. C.; Lovenberg, W. In *Essays in Neurochemistry and Neuropharmacology*; Youdim, M. B. H., Lovenberg, W., Sharman, D. F., Lagnado, J. R., Eds.; Wiley: New York, 1980; Vol. 4, pp 163–209.
- (4) Villafranca, J. J. In *Copper Proteins*; Spiro, T. G., Ed.; Wiley: New York, 1981; pp 263–289.
- (5) Ljones, T.; Skotland, T. In *Copper Proteins and Copper Enzymes*; Lontie, R., Ed.; CRC Press: Boca Raton, FL, 1986; Vol. 2, pp 131–157.
- (6) Terland, O.; Flatmark, T. *FEBS Lett.* **1975**, *59*, 52.
- (7) Klinman, J. P. *Chem. Rev.* **1996**, *96*, 2541.
- (8) Stubbe, J.; van der Donk, W. A. *Chem. Rev.* **1998**, *98*, 705.
- (9) Kruse, L. I.; DeWolf, W. E., Jr.; Chambers, P. A.; Goodhart, P. J. *Biochemistry* **1986**, *25*, 7271.

- (10) Li, B.; Tsing, S.; Kosaka, A. H.; Nguyen, B.; Osen, E. G.; Bach, C.; Chan, H.; Barnett, J. *Biochem. J.* **1996**, *313*, 57.
- (11) Battersby, A. R.; Sheldrake, P. W.; Staunton, J.; Williams, D. C. *J. Chem. Soc., Perkin Trans. 1* **1976**, 1056.
- (12) Stewart, L. C.; Klinman, J. P. *Annu. Rev. Biochem.* **1988**, *57*, 551.
- (13) Ash, D. E.; Papadopoulos, N. J.; Colombo, G.; Villafranca, J. J. *J. Biol. Chem.* **1984**, *259*, 3395.
- (14) Klinman, J. P.; Krueger, M.; Brenner, M.; Edmondson, D. E. *J. Biol. Chem.* **1984**, *259*, 3399.
- (15) McCracken, J.; Desai, P. R.; Papadopoulos, N. J.; Villafranca, J. J.; Peisach, J. *Biochemistry* **1988**, *27*, 4133.
- (16) Brenner, M. C.; Klinman, J. P. *Biochemistry* **1989**, *28*, 4664.

Scheme 2



failed to detect backscattering between the copper centers in contrast to hemocyanin and tyrosinase,^{18,19} in which the two copper atoms are antiferromagnetically coupled. The two copper atoms of DBM are not chemically equivalent and are considered to perform different functions in the catalysis. One copper site of DBM (Cu_A) plays an important role in the binding of ascorbate and the electron transfer from ascorbate to the other copper site (Cu_B), which functions as the active site for the substrate binding and the oxygen insertion into substrate.^{16,20,21} EXAFS measurements^{17,22,23} indicated that Cu_A is coordinated by three histidine ligands to the DBM backbone, whereas Cu_B is coordinated by two histidines and one methionine.

A proposed mechanism for O–O bond activation in DBM is shown in Scheme 2. At first, ascorbate reduces both copper atoms to produce a noncoupled $\text{Cu(I)}_A\text{Cu(I)}_B$, which is stable in the absence of substrate on a second time scale.¹⁶ Dioxygen is incorporated into the Cu(I)_B site to give a Cu(II)-superoxo species, followed by an electron transfer from Cu_A to Cu_B , resulting in a Cu(I)-superoxo species. A $\text{Cu(II)-hydroperoxo}$ species is next formed by the protonation of the Cu(I)-superoxo species.^{14,16,24} Finally the $\text{Cu(II)-hydroperoxo}$ species abstracts a hydrogen atom from a key tyrosine residue near the active site of DBM to produce a Cu(III)-oxo species, a water molecule, and a tyrosyl radical.²⁵ This proposal is in good agreement with ¹⁸O kinetic isotope effects with several substrate analogues which indicate that the cleavage of the O–O bond to takes place prior to the hydrogen-atom abstraction from dopamine. Although mononuclear Cu(III)-oxo species have not yet been captured experimentally, its formation can be promoted by the production of a water molecule. However, the geometries and energies of these species along the reaction pathway have not yet been determined.

DBM is similar in many respects to peptidylglycine α -hydroxylating monooxygenase (PHM; EC 1.14.17.3),²⁶ the X-ray structure of which was solved at 1.85 Å resolution.^{27,28} PHM also contains two copper atoms, Cu_A and Cu_B , separated by a solvent pocket at a distance of 11 Å. The Cu_A site is responsible for ascorbate binding and electron transfer, while the Cu_B site is involved in the hydrogen-atom abstraction from the α -carbon of the C-terminal glycine concomitant with the reductive cleavage of dioxygen. These similarities can derive from the high amino acid identity of 30% in the catalytic core,²⁹ which is a piece of evidence for the close evolutionary relationship between the two enzymes. Recently, geometric and electronic features of the active sites of both the Cu_A and Cu_B centers in PHM were characterized.³⁰ Chen and Solomon³¹ proposed a mechanism for the hydroxylation of formylglycine by a side-on Cu(II)-superoxo species of PHM using density functional theory (DFT) calculations. The activation barrier for the hydrogen-atom abstraction by the $\text{Cu(II)-hydroperoxo}$ species was calculated to be 37 kcal/mol, while that by the Cu(II)-superoxo species was calculated to be 14 kcal/mol.

In a previous paper,³² we reported reaction features of the copper-superoxo, -hydroperoxo, and -oxo species. Since the X-ray structure of DBM has not yet been successfully determined, we constructed a whole-enzyme model of DBM on the basis of the crystal structure of PHM using homology-modeling techniques. Then we performed quantum mechanical/molecular mechanical (QM/MM) calculations to refine the structure involving complex hydrogen-bonding interactions between the three kinds of active oxygen species and substrate in the catalytic core. DFT calculations using small-cluster models extracted from the QM region showed that the copper-superoxo, -hydroperoxo, and -oxo species can abstract a hydrogen atom at the benzylic position of dopamine with activation energies of 17, 40, and 4 kcal/mol, respectively. The result leads us to conclude that the oxo species should mediate the catalytic function of DBM. However, optimized structures of these oxidants in the small-cluster model calculations are somewhat different from those in the whole-enzyme calculations in that the small-cluster model structures are seriously perturbed by fictitious hydrogen-bonding interactions that are not seen in the QM/MM optimized structures. Since the hydrogen bond should significantly affect the energetic profile, in the present study we try to better understand the enzymatic processes of the copper-superoxo and -oxo species using whole-enzyme QM/MM calculations and look at how the protein environment of DBM affects the reaction profile. Here we do not consider

- (17) Scott, R. A.; Sullivan, R. J.; DeWolf, W. E., Jr.; Dolle, R. E.; Kruse, L. I. *Biochemistry* **1988**, *27*, 5411.
- (18) Solomon, E. I.; Sundaram, U. M.; Machonkin, T. E. *Chem. Rev.* **1996**, *96*, 2563.
- (19) Solomon, E. I.; Chen, P.; Metz, M.; Lee, S.-K.; Palmer, A. E. *Angew. Chem., Int. Ed.* **2001**, *40*, 4570.
- (20) Blackburn, N. J.; Pettingill, T. M.; Seagraves, K. S.; Shigetani, R. T. *J. Biol. Chem.* **1990**, *265*, 15383.
- (21) Pettingill, T. M.; Strange, R. W.; Blackburn, N. J. *J. Biol. Chem.* **1991**, *266*, 16996.
- (22) Blackburn, N. J.; Hasnain, S. S.; Pettingill, T. M.; Strange, R. W. *J. Biol. Chem.* **1991**, *266*, 23120.
- (23) Reedy, B. J.; Blackburn, N. J. *J. Am. Chem. Soc.* **1994**, *116*, 1924.
- (24) Miller, S. M.; Klinman, J. P. *Biochemistry* **1985**, *24*, 2114.
- (25) Tian, G.; Berry, J. A.; Klinman, J. P. *Biochemistry* **1994**, *33*, 226.

- (26) Kulathila, R.; Merkler, K. A.; Merkler, D. *J. Nat. Prod. Rep.* **1999**, *16*, 145.
- (27) Prigge, S. T.; Kolhekar, A. S.; Eipper, B. A.; Mains, R. E.; Amzel, L. M. *Science* **1997**, *278*, 1300.
- (28) Prigge, S. T.; Eipper, B. A.; Mains, R. E.; Amzel, L. M. *Science* **2004**, *304*, 864.
- (29) Southan, C.; Kruse, L. I. *FEBS Lett.* **1989**, *255*, 116.
- (30) Chen, P.; Bell, J.; Eipper, B. A.; Solomon, E. I. *Biochemistry* **2004**, *43*, 5735.
- (31) Chen, P.; Solomon, E. I. *J. Am. Chem. Soc.* **2004**, *126*, 4991.
- (32) Kamachi, T.; Kihara, N.; Shiota, Y.; Yoshizawa, K. *Inorg. Chem.* **2005**, *44*, 4226.

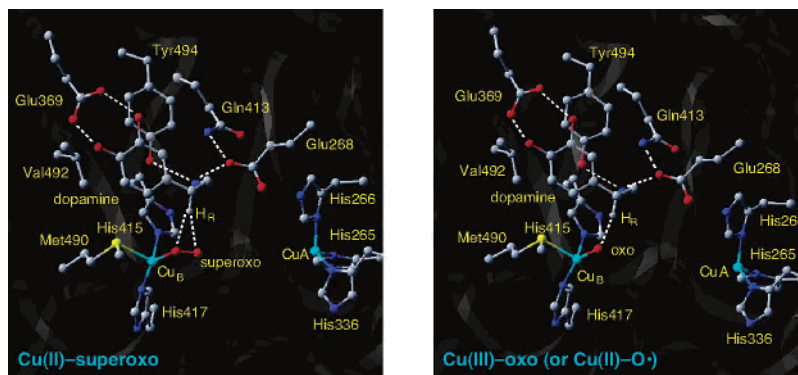


Figure 1. QM/MM optimized whole-enzyme DBM models with 4700 atoms.

the copper-hydroperoxo species because its reactivity is not sufficient for the C–H bond activation.^{31,32}

2. Method of Calculation

We obtained the amino acid sequences of DBM and PHM from SwissProt DataBank;³³ the sequence identity between DBM and PHM is 29.5%. A three-dimensional model of rat DBM was constructed with the crystal structure coordinates of PHM (Protein Databank IOPM) from the modeling program available at <http://www.cbs.dtu.dk/services/CPHmodels/>.³⁴ To make a whole-enzyme model for the QM/MM calculations, missing hydrogen atoms were added, and then initial MM minimization was performed while the QM region was fixed. Merz–Kollman electrostatic potential charges³⁵ taken from small-cluster model calculations were used as the point charges of the QM region for initial MM optimization. The obtained model with about 4700 atoms was used as an initial structure for the QM/MM calculations with the two-layer ONIOM (IMOMM) method³⁶ implemented in the Gaussian 03 program.³⁷ A specified region around the active center was calculated with a QM method, while the rest of the protein was calculated with an

MM method. The QM region describes the essential bond-cleavage and -formation processes in the enzyme, while the MM region promotes interactions with the QM region through partial charges and van der Waals forces of atoms in the MM region. Here we chose the Cu_B atom, the superoxo and oxo ligands, substrate, and neighboring amino acid residues (His415, His417, and Met490) as the QM region. At the QM/MM border, atoms in the MM region bound to an atom in the QM region were replaced by hydrogen atoms in the QM region of the QM/MM calculation. QM calculations were performed with the B3LYP DFT method, which consists of the Slater exchange, the Hartree–Fock exchange, the exchange functional of Becke,³⁸ the correlation functional of Lee, Yang, and Parr (LYP),³⁹ and the correlation functional of Vosko, Wilk, and Nusair.⁴⁰ We used the triple- ζ -valence (TZV) basis set⁴¹ for the Cu_B atom, the D95* basis set⁴² for the superoxo and oxo ligands and the atoms that directly coordinate to the Cu_B atom, and the D95 basis set for other atoms. The method of choice for MM calculations is the Amber96 force field.⁴³ Figure 1 shows optimized structures for the whole-enzyme models of Cu(II)–superoxo and Cu(III)–oxo (or Cu(II)–O•).

These structures were obtained with optimization convergence criteria of 4.5×10^{-4} hartree per bohr for the gradient of energy and 3.0×10^{-4} hartree per bohr for the root-mean-square gradient of energy.

3. Results and Discussion

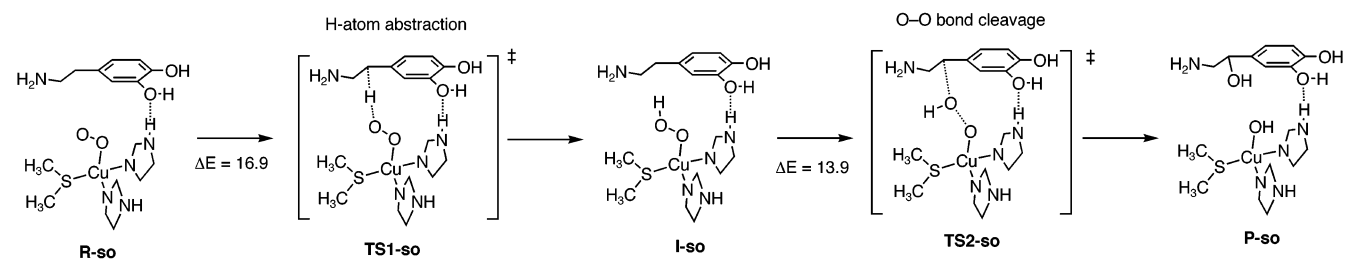
3.1. Overview of the Small-Cluster Model Calculations.

Let us first look at reaction profiles for dopamine hydroxylation that we obtained previously³² using a small-cluster model that mimics the coordination sphere of the active site before discussing the protein environmental effects on the overall reaction profiles using a whole-enzyme model. Figure 2 shows essential features of the calculated geometries for the reactant, product, intermediates, and transition states for dopamine hydroxylation using a small cluster that models the Cu(II)–superoxo species in the antiferromagnetically coupled singlet state. In the initial stages of the reaction, a dopamine molecule is bound to the Cu(II)–superoxo species

- (33) Bairoch, A.; Boeckmann B. *Nucleic Acids Res.* **1992**, *20*, 2019.
 (34) Lund, O.; Nielsen, M.; Lundegaard, C.; Worning P. Abstract at the CAPS5 conference A102, 2002.
 (35) (a) Singh, U. C.; Kollman, P. A. *J. Comput. Chem.* **1984**, *5*, 129. (b) Besler, B. H.; Merz, K. M. Jr.; Kollman, P. A. *J. Comput. Chem.* **1990**, *11*, 431.
 (36) (a) Maseras, F.; Morokuma, K. *J. Comput. Chem.* **1995**, *16*, 1170. (b) Humbel, S.; Sieber, S.; Morokuma, K. *J. Chem. Phys.* **1996**, *105*, 1959. (c) Matsubara, T.; Sieber, S.; Morokuma, K. *Int. J. Quantum Chem.* **1996**, *60*, 1101. (d) Svensson, M.; Humbel, S.; Froese, R. D. J.; Matsubara, T.; Sieber, S.; Morokuma, K. *J. Phys. Chem.* **1996**, *100*, 19357. (e) Svensson, M.; Humbel, S.; Morokuma, K. *J. Chem. Phys.* **1996**, *105*, 3654. (f) Dapprich, S.; Komáromi, I.; Byun, K. S.; Morokuma, K.; Frisch, M. J. *J. Mol. Struct. (THEOCHEM)* **1999**, *461–462*, 1. (g) Vreven, T.; Morokuma, K. *J. Comput. Chem.* **2000**, *21*, 1419.
 (37) Frisch, M. J.; Trucks, G. W.; Schlegel, H. B.; Scuseria, G. E.; Robb, M. A.; Cheeseman, J. R.; Montgomery, J. A., Jr.; Vreven, T.; Kudin, K. N.; Burant, J. C.; Millam, J. M.; Iyengar, S. S.; Tomasi, J.; Barone, V.; Mennucci, B.; Cossi, M.; Scalmani, G.; Rega, N.; Petersson, G. A.; Nakatsuji, H.; Hada, M.; Ehara, M.; Toyota, K.; Fukuda, R.; Hasegawa, J.; Ishida, M.; Nakajima, T.; Honda, Y.; Kitao, O.; Nakai, H.; Klene, M.; Li, X.; Knox, J. E.; Hratchian, H. P.; Cross, J. B.; Bakken, V.; Adamo, C.; Jaramillo, J.; Gomperts, R.; Stratmann, R. E.; Yazyev, O.; Austin, A. J.; Cammi, R.; Pomelli, C.; Ochterski, J. W.; Ayala, P. Y.; Morokuma, K.; Voth, G. A.; Salvador, P.; Dannenberg, J. J.; Zakrzewski, V. G.; Dapprich, S.; Daniels, A. D.; Strain, M. C.; Farkas, O.; Malick, D. K.; Rabuck, A. D.; Raghavachari, K.; Foresman, J. B.; Ortiz, J. V.; Cui, Q.; Baboul, A. G.; Clifford, S.; Cioslowski, J.; Stefanov, B. B.; Liu, G.; Liashenko, A.; Piskorz, P.; Komaromi, I.; Martin, R. L.; Fox, D. J.; Keith, T.; Al-Laham, M. A.; Peng, C. Y.; Nanayakkara, A.; Challacombe, M.; Gill, P. M. W.; Johnson, B.; Chen, W.; Wong, M. W.; Gonzalez, C.; Pople, J. A. *Gaussian 03*; Gaussian, Inc.: Wallingford, CT, 2004.

- (38) (a) Becke, A. D. *Phys. Rev. A* **1988**, *38*, 3098. (b) Becke, A. D. *J. Chem. Phys.* **1993**, *98*, 5648.
 (39) Lee, C.; Yang, W.; Parr, R. G. *Phys. Rev. B* **1988**, *37*, 785.
 (40) Vosko, S. H.; Wilk, L.; Nusair, M. *Can. J. Phys.* **1980**, *58*, 1200.
 (41) Schäfer, A.; Huber, C.; Ahlrichs, R. *J. Chem. Phys.* **1994**, *100*, 5829.
 (42) Dunning, T. H.; Hay, P. J. In *Modern Theoretical Chemistry*; Schaefer, H. F., III, Ed.; Plenum: New York, 1976; Vol. 3, p 1.
 (43) Cornell, W. D.; Cieplak, P.; Bayly, C. I.; Gould, I. R.; Merz, K. M., Jr.; Ferguson, D. M.; Spellmeyer, D. C.; Fox, T.; Caldwell, J. W.; Kollman, P. A. *J. Am. Chem. Soc.* **1995**, *117*, 5179.

Cu(II)-superoxo



Cu(III)-oxo or Cu(II)-O•

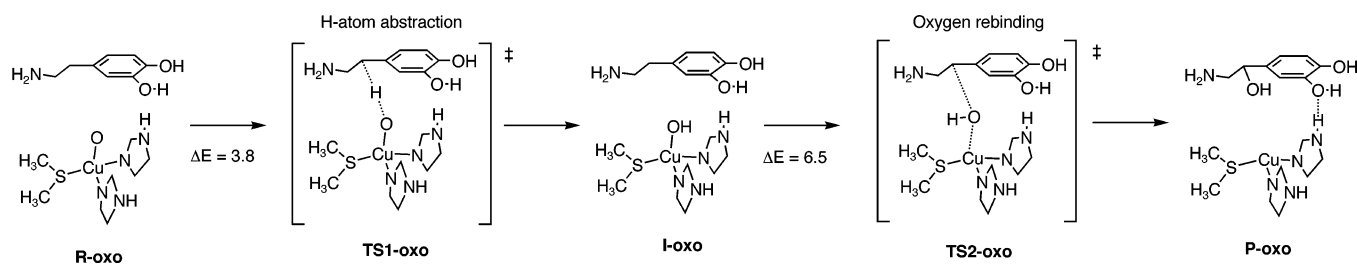


Figure 2. Mechanisms for dopamine hydroxylation mediated by the Cu(II)-superoxo and Cu(III)-oxo species of DBM based on small-model calculations. Note that a fictitious hydrogen-bonding interaction is formed between an imidazole ligand and substrate. Activation energies in are given in kilocalories per mole.

to form the reactant complex (**R-so**). The binding energy for **R-so** was predicted to be 11.8 kcal/mol, but it was overestimated because of the fictitious hydrogen-bonding interaction between the OH group of dopamine and an imidazole ligand that is not observed in the whole-enzyme QM/MM calculations, as seen later in this paper. A calculated activation barrier for the hydrogen-atom abstraction via the first transition state (**TS1-so**) is 16.9 kcal/mol when measured from **R-so**. The substrate radical in the resultant radical intermediate (**I-so**) recombines with the distal oxygen of the hydroperoxo ligand to form the product complex (**P-so**) via the second transition state for the rebound process (**TS2-so**). The barrier height for **TS2-so** is 9.7 kcal/mol when it is measured from **I-so**. The release of norepinephrine from **P-so** leads to the final product.

In dopamine hydroxylation mediated by the Cu(III)-oxo species, which can also be viewed as Cu(II)-O•, a dopamine molecule comes into contact with the Cu(III)-oxo species to form the reactant complex (**R-oxo**), as shown in Figure 2. The binding energies for **R-oxo** in the triplet and singlet states were calculated to be 8.3 and 8.8 kcal/mol, respectively. The triplet state lies 4.6 kcal/mol below the singlet state in the Cu(III)-oxo species. The pro-R hydrogen atom of dopamine is abstracted by the oxo ligand of the Cu(III)-oxo species via the first transition state (**TS1-oxo**) to lead to the radical intermediate (**I-oxo**). The activation energy for this process is only 3.8 (0.8) kcal/mol in the triplet (singlet) state. From now on, we list the energy values for the singlet state in parentheses next to the corresponding values for the triplet state. This low barrier height indicates that the Cu(III)-oxo species has rather high reactivity toward dopamine compared to the Cu(II)-superoxo species. The calculated activation energy for the recombination of the substrate radical (**TS2-oxo**) is 51.4 and 6.5 kcal/mol in the triplet and singlet states, respectively. **TS2-oxo** for the

rebound step is 31.0 kcal/mol higher than that for the hydrogen-atom abstraction on the triplet potential surface. If we assume that the reaction occurs only on the triplet potential energy surface, this result might be inconsistent with observed large kinetic isotope effects,⁴⁴ which suggest the involvement of hydrogen-atom transfer in the rate-determining step. Detailed calculations suggest that **I-oxo** and **P-oxo** have different spin multiplicities in their lower-energy states and that the reaction should involve a spin-inversion electronic process⁴⁵ near the crossing region between the triplet and singlet potential energy surfaces. Spin-orbit coupling plays an important role in spin-inversion electronic processes in transition-metal-mediated reactions and spin-crossover phenomena.⁴⁶ Assuming that the spin inversion takes place from the triplet state to the singlet state in the vicinity of **I-oxo**, the overall reaction by the Cu(III)-oxo species is highly exothermic, and the transition states involved are low-lying; therefore this reaction should easily take place. The small-cluster model calculations that neglect protein-environmental effects are useful as the first step toward our understanding of the enzymatic function of DBM.

3.2. Key Amino Acid Residues in the Catalytic Core.

Since the small-model calculations include the fictitious hydrogen-bonding interactions that can lead to an erroneous energy profile for the reaction, let us look at important amino acid residues at the active site. The constructed whole-enzyme model of DBM is composed of two domains. Figure 1 shows that domain 1 involves Cu_A coordinated by the δ -nitrogen of three histidine residues (His265, His266, and

(44) Miller, S. M.; Klinman, J. P. *Biochemistry* **1983**, *22*, 3091.

(45) (a) Fiedler, A.; Schröder, D.; Shaik, S.; Schwarz, H. *J. Am. Chem. Soc.* **1994**, *116*, 10734. (b) Shaik, S.; Danovich, D.; Fiedler, A.; Schröder, D.; Schwarz, H. *Helv. Chim. Acta* **1995**, *78*, 1393. (c) Schröder, D.; Shaik, S.; Schwarz, H. *Acc. Chem. Res.* **2000**, *33*, 139.

(46) (a) Shiota, Y.; Yoshizawa, K. *J. Chem. Phys.* **2003**, *118*, 5872. (b) Kondo, M.; Yoshizawa, K. *Chem. Phys. Lett.* **2003**, *372*, 519.

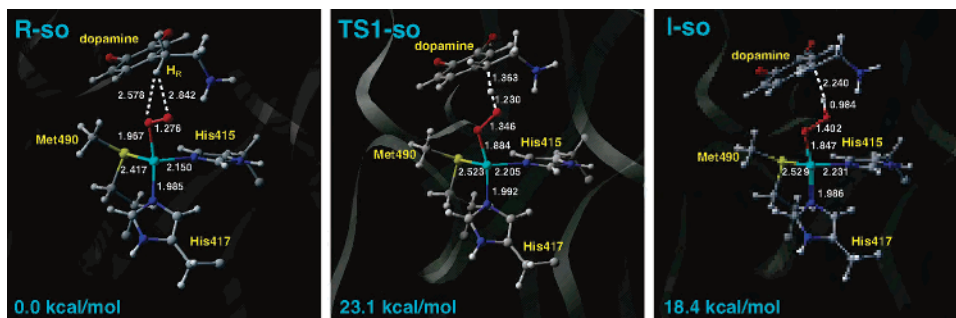


Figure 3. Computed energetic and structural changes in the hydrogen-atom abstraction by the Cu(II)–superoxo species in the antiferromagnetically coupled singlet state. Bond distances in units of angstroms.

His336), while domain 2 involves Cu_B coordinated by the ϵ -nitrogen of two histidine residues (His415 and His417) and by a methionine sulfur of Met490. The coordination spheres of the Cu sites predicted by the homology modeling are consistent with spectroscopic measurements^{17,22,23} indicating that the Cu sites contain two or three histidine N atoms and one methionine S atom. There is a cleft that is fully accessible to solvent which links the two copper sites; they are about 10 Å apart. The amino acid residues at the computed active site of DBM and the observed active site of PHM are in good agreement.⁴⁷ We placed a dopamine molecule at the active site of DBM, positioning the reactive β -carbon of dopamine at the same position as the reactive α -carbon of a peptidylglycine molecule bound to PHM. This whole-enzyme model of DBM shows that a complex hydrogen-bonding network with surrounding amino acid residues (Glu268, Glu369, and Tyr494) anchors the substrate. The Tyr494 residue that is conserved in all DBM sequences plays an important role in the enzymatic reaction via the hydrogen-bonding interaction with the amino group of dopamine as the Tyr318 residue in PHM forms a hydrogen bond with the substrate glycine. The Glu268 residue is also hydrogen-bonded to the amino group of dopamine. This glutamic acid is conserved in all DBM sequences, but it is replaced in PHM with leucine that cannot interact with substrate. Instead of the leucine residue, the Arg240 in PHM is tightly bonded to substrate in a manner similar to that of Glu268 in the DBM model. The Glu369 residue prevents the formation of the fictitious hydrogen bond between the His415 residue and the hydroxyl group of dopamine in the small-cluster model calculations. These hydrogen-bonding networks make the pro-R hydrogen atom come into close contact with the active site of DBM for the stereospecific hydrogen-atom abstraction.

3.3. Reactivity of the Cu(II)–Superoxo Species in the Protein Environment. In a previous study³² we looked at the structure of the Cu(II)–superoxo species in the protein environment of DBM using the QM/MM method. Dioxygen can bind into the vacant coordination site of the catalytic core in an end-on or side-on manner, depending on level of theory used. The QM/MM optimizations located both side-on and end-on Cu(II)–superoxo species in the closed-shell singlet state, but we found the energy minimum only for the end-on Cu(II)–superoxo species in the antiferromag-

Table 1. Calculated Mulliken Charges and Spin Densities of Dopamine, the Cu Atom, and Its Ligands for Dopamine Hydroxylation by the Cu(II)–Superoxo Species^a

	R-so	TS1-so	I-so
Cu	0.9 (0.3)	0.8 (0.2)	0.9 (0.3)
O ₂	−0.2 (−0.4)	−0.2 (0.4)	−0.3 (0.5)
His415	0.1 (0.0)	0.1 (0.0)	0.1 (0.0)
His417	0.1 (0.0)	0.1 (0.0)	0.1 (0.0)
Met490	0.2 (0.0)	0.1 (0.0)	0.1 (0.1)
dopamine	0.0 (0.0)	0.1 (−0.6)	0.0 (−1.0)

^a Values in parentheses are spin densities.

netically coupled singlet state. This end-on species is 10.7 (17.5) kcal/mol lower than the side-on (end-on) Cu(II)–superoxo species in the closed-shell singlet state. This result is fully consistent with the recent X-ray structural analysis of PHM, in which dioxygen is bound to Cu_B in an end-on mode.²⁸ Figure 3 shows optimized geometries of the reaction species for the hydrogen-atom abstraction by the Cu(II)–superoxo species in the protein environment.

Calculated atomic charges and spin densities are listed in Table 1. In the QM/MM optimized structure of the end-on Cu(II)–superoxo species, the spin densities on the Cu atom and the superoxo ligand are 0.3 and −0.4, respectively, which confirms that the net diamagnetism of the Cu(II)–superoxo complex is attributed to the antiferromagnetic coupling between the two units of spin on the Cu atom and the superoxo ligand. The bond distances of Cu–O (distal), Cu–O (proximal), and O–O are 2.671, 1.967, and 1.276 Å, respectively. This O–O bond length is typical of superoxo ligands of about 1.3 Å. A rotation of the distal oxygen atom by 108.8° around the Cu–O bond places the distal oxygen atom to be located 1.569 Å from the pro-R hydrogen atom. This geometrical arrangement can induce a significant interaction between the distal oxygen atom and the hydrogen atom to be abstracted, which triggers the stereospecific hydrogen-atom abstraction.²⁸

Table 2 lists a computed energy profile for the hydrogen-atom abstraction by the Cu(II)–superoxo species of DBM in the antiferromagnetically coupled singlet state in the protein environment as a function of the distance between the distal oxygen atom and the pro-R hydrogen atom. We obtained the energies of intermediate points using partial optimizations under the constraint of the O–H bond. The relative energies of these points are increased by the shortening of the O–H bond, and the total profile reaches a maximum value of 23.1 kcal/mol at the O–H bond distance

(47) Prigge, S. T.; Mains, R. E.; Eipper, B. A.; Amzel, L. M. *Cell. Mol. Life Sci.* **2000**, *57*, 1236.

Table 2. Geometries and Energies of Selected Points, 1–8, along the H-Atom Abstraction Process by the Cu(II)–superoxo Species in the Singlet State

	point							
	1	2	3	4	5	6	7	8
C–H	1.099	1.307	1.343	1.363	1.387	1.441	1.472	2.240
O–H	2.842	1.260 ^a	1.240 ^a	1.230 ^a	1.220 ^a	1.200 ^a	1.190 ^a	0.984
energy	0.0	22.8	23.0	23.1	23.0	23.0	22.8	18.4

^a The O–H distance is constrained during a geometry optimization. All distances and energies are in angstroms and kilocalories per mole, respectively. Points 1 and 8 are fully optimized structures.

of 1.230 Å. This maximum point corresponds to the transition state for the hydrogen-atom abstraction (**TS1–so**). This process is accompanied by the activation of the C–H bond of dopamine and the O–O bond of the superoxo ligand; the C–H and O–O bonds of the transition state were calculated to be 1.363 and 1.346 Å, respectively. After **TS1–so** is passed, the shortening of the O–H bond results in the formation of the radical intermediate (**I–so**). The C–H bond distance varies from 1.099 to 2.240 Å and the O–H bond from 2.842 to 0.984 Å in the course of the hydrogen-atom abstraction, while the Cu–N and Cu–S bonds remain almost unchanged. The relative energy of the fully optimized radical intermediate is 18.4 kcal/mol when measured from the reactant complex. The calculated spin density on the substrate radical is –1.0, which confirms the radical character of the intermediate indicated by the negative Hammett reaction constant, ρ , value.²⁴

The hydrogen-bonding interactions between dopamine and the important amino acid residues (Glu268, Glu369, and Tyr494) are retained throughout the hydrogen-atom abstraction. These interactions tightly fix the dopamine molecule and the produced dopamine radical at the substrate-binding site. For example, the distance between the Cu atom and the β -carbon of dopamine remains essentially unchanged in this process: 5.117 Å for the Cu(II)–superoxo species, 4.906 Å for **TS1–so**, and 5.113 Å for **I–so**. On the other hand, the substrate easily rotates and directly interacts with the superoxo ligand and imidazole ligands via a relatively strong hydrogen bond in the previous small-cluster model calculations.³² The distance between the Cu atom and the β -carbon of dopamine was significantly changed by these fictitious hydrogen-bonding interactions: 6.572 Å for the Cu(II)–superoxo species, 4.731 Å for **TS1–so**, and 5.185 Å for **I–so**. Thus, the surrounding amino acid residues in the hydrogen-atom abstraction control the orientation of the dopamine molecule, and therefore the energetics from the previous small-cluster model calculations should be reevaluated. A calculated activation energy for this step in the protein environment of DBM is 23.1 kcal/mol, which is 6.2 kcal/mol higher than that from the small-cluster model. These results demonstrate that the inclusion of the hydrogen-bonding interactions between substrate and the surrounding amino acid residues is essential for a better description of the hydrogen-atom abstraction in the protein environment. This activation barrier is rather high compared to the activation barrier of 5.4 kcal/mol in the oxo-mediated pathway, as discussed later in this work. Moreover, the

hydrogen atom once abstracted by the superoxo ligand easily comes back to the substrate radical to form dopamine again because of the high relative energy of **I–so**, which is inconsistent with the experimental failure⁴⁴ to observe the reformation of dopamine from enzyme-bound intermediate or product. For these reasons, we think that the hydroxylation of dopamine by the Cu(II)–superoxo species is not favorable.

3.4. Reactivity of the Cu(III)–Oxo Species in the Protein Environment. Previously we studied the conversion of methane to methanol by the first-row MO⁺ complexes in detail,⁴⁸ in which M is Sc, Ti, V, Cr, Mn, Fe, Co, Ni, and Cu. General profiles of the energy diagrams for the reactions indicated that methane hydroxylation efficiently takes places with the late MO⁺ complexes (M = Fe, Ni, and Cu). A calculated Cu–O bond length of 1.758 Å is rather long in comparison to those of the other MO⁺ complexes, and therefore, this species can be viewed as a Cu(II)–O[•] species. The methane hydroxylation by the CuO⁺ complex is highly exothermic (–50.0 kcal/mol) as a result of the spin crossover from the triplet state to the singlet state. From these results, we expect that the possible Cu(III)–oxo (or Cu(II)–O[•]) species at the catalytic active site of DBM should make a good mediator for dopamine hydroxylation. A computed Cu–O binding energy for DBM is 41.2 kcal/mol, which is larger than the 37.6 kcal/mol value for the bare CuO⁺ complex, because of the surrounding amino acid residues.

The triplet and singlet potential energy surfaces of dopamine hydroxylation by the Cu(III)–oxo species are close lying in energy in the initial stages of the reaction. The QM/MM calculations tell us that the energy separation between the two spin states is increased because of the histidine and methionine ligands; the ground triplet state lies 6.5 kcal/mol below the singlet state in the QM/MM calculations. The spins on the Cu atom and the oxo ligand are arranged in ferromagnetic and antiferromagnetic manners in the triplet and singlet states, respectively. The spin density of the Cu(III)–oxo species is heavily localized on the CuO moiety and the spin densities of the Cu atom and the oxo ligand are 0.5 (0.4) and 1.3 (–0.6) in the triplet (singlet) state, respectively. Therefore this copper–oxygen species can reasonably be viewed as a resonance hybrid between Cu(III)–oxo and Cu(II)–O[•]. The Cu(III)–oxo species, Cu–O(oxo), Cu–N(His415), Cu–N(His417), and Cu–S(Met490) bond lengths in the optimized structure are 1.779 (1.788), 2.115 (2.136), 1.986 (1.972), and 2.441 (2.432) Å in the triplet (singlet) state, respectively. The long Cu–O bond distance implies that the high reactivity of the Cu(III)–oxo species is retained in the protein environment.

Figure 4 shows the optimized geometries of the intermediates (**R–oxo** and **I–oxo**) and transition states (**TS1–oxo** and **TS2–oxo**) for the hydrogen-atom abstraction and the rebound step in the protein environment of DBM. This reaction is an extension of the so-called oxygen rebound

(48) (a) Yoshizawa, K.; Shiota, Y.; Yamabe, T. *Chem.–Eur. J.* **1997**, *3*, 1160. (b) Yoshizawa, K.; Shiota, Y.; Yamabe, T. *J. Am. Chem. Soc.* **1998**, *120*, 564. (c) Shiota, Y.; Yoshizawa, K. *J. Am. Chem. Soc.* **2000**, *122*, 12317.

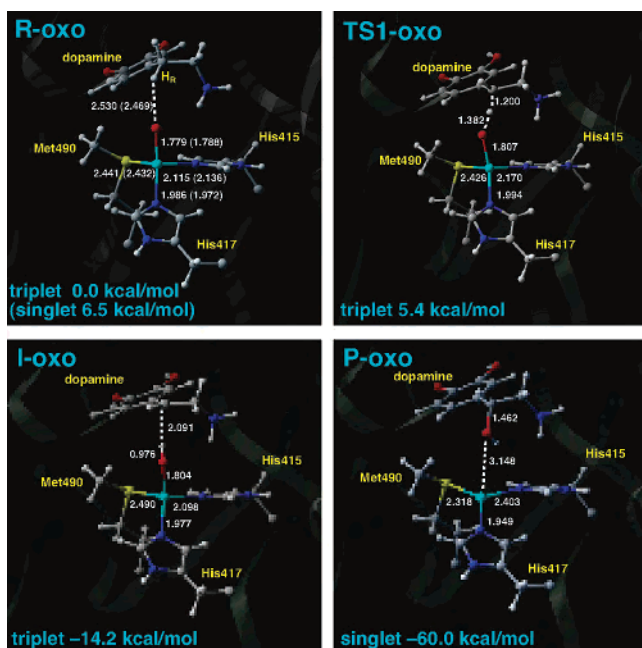


Figure 4. Computed energetic changes in the hydrogen-atom abstraction and the oxygen rebound step by the Cu(III)–oxo species. Bond distances in units of angstroms.

Table 3. Calculated Mulliken Charges and Spin Densities of Dopamine, the Cu Atom, and Its Ligands for Dopamine Hydroxylation by the Cu(III)–Oxo Species^a

	R–oxo		TS1–oxo	I–oxo	P–oxo
	triplet	singlet	triplet	triplet	singlet
Cu	1.0 (0.5)	1.0 (0.4)	1.0 (0.4)	1.0 (0.5)	0.7 (0.0)
O	−0.4 (1.3)	−0.5 (−0.6)	−0.6 (1.0)	−0.4 (0.4)	−0.2 (0.0)
His415	0.1 (0.1)	0.1 (0.0)	0.1(0.0)	0.1 (0.0)	0.1 (0.0)
His417	0.1 (0.0)	0.2 (0.0)	0.1 (0.0)	0.1 (0.0)	0.1 (0.0)
Met490	0.2 (0.1)	0.2 (0.0)	0.2 (0.1)	0.1 (0.1)	0.1 (0.0)
dopamine	0.0 (0.0)	0.0 (0.0)	0.3 (0.4)	0.0 (1.0)	0.2 (0.0)

^aValues in parentheses are spin densities.

mechanism⁴⁹ to a copper-based monooxygenase. Table 3 lists computed atomic charges and spin densities of these reaction species. To determine the energy of the C–H bond activation process by the Cu(III)–oxo species, we defined several intermediate steps from the Cu(III)–oxo species (the first point) to **I–oxo** (the last point) using partial optimizations with the constraint of the benzylic C–H bond of dopamine.

Table 4 lists key geometrical features and energies of eight selected points along the reaction coordinate for the hydrogen-atom abstraction in the triplet state. A calculated activation energy for this step is 5.4 kcal/mol, which is as high as that in the small-cluster model³² without protein environment. The transition state for this hydrogen-atom abstraction has an O–H bond length of 1.382 Å and a C–H bond of length of 1.200 Å; these bond distances as well as the linear O–H–C array are nearly identical to those of the corresponding **TS1-oxo** in the small-cluster model. Thus, in the oxo-mediated reaction, the protein environment does not significantly affect the activation barrier and the key parameters of the transition state in contrast to those for the

Table 4. Geometries and Energies of Selected Points, 1–8, along the H-Atom Abstraction Process by the Cu(III)–Oxo Species in the Triplet State

	point							
	1	2	3	4	5	6	7	8
C–H	1.097	1.180 ^a	1.190 ^a	1.200 ^a	1.210 ^a	1.260 ^a	1.300 ^a	2.091
O–H	2.530	1.636	1.458	1.382	1.305	1.196	1.147	0.976
energy	0.0	4.8	5.3	5.4	4.7	3.3	1.6	−14.2

^aThe C–H distance is constrained during a geometry optimization. All distances and energies are in angstroms and kilocalories per mole, respectively. Points 1 and 8 are fully optimized structures.

superoxo-mediated hydrogen-atom abstraction. This result is rationalized by looking at the hydrogen bonds between dopamine and the small-cluster models in the hydrogen-atom abstraction. In the oxo-mediated pathway, the orientation of dopamine remains almost unchanged in the course of the hydrogen-atom abstraction, while in the superoxo-mediated pathway, the orientation of dopamine is significantly changed because of the fictitious hydrogen-bonding interaction.³² However, in the whole-enzyme models, dopamine is tightly fixed in a proper position by the surrounding hydrogen-bonding network in both cases, and thus the incorrect energetics of the small-cluster model calculations for the Cu(II)–superoxo species are improved in the whole-enzyme model. We therefore should take the hydrogen-bonding interactions between the substrate and surrounding amino acid residues into consideration for a better description of enzymatic reactions in general.

The second half of the reaction starts from the resultant radical intermediate **I–oxo**. A computed energy of **I–oxo** in the triplet state is −14.2 kcal/mol relative to the reactant complex. The carbon radical center of this intermediate weakly interacts with the OH ligand at a distance of 2.091 Å. The spin densities of the Cu atom and dopamine radical were calculated to be 0.5 and 1.0, respectively. QM/MM calculations demonstrate that the subsequent recombination of the dopamine radical requires a high activation energy of 38.8 kcal/mol on the triplet potential energy surface because of a change in the electronic configuration of the copper atom (i.e., the reduction of the copper atom from +2 to +1). The ground state of the Cu(I) atom is well-known to have a closed-shell d^{10} configuration, and the triplet d^9s^1 excited state is 66 kcal/mol higher than the singlet ground state.⁵⁰ Thus, the reason for the high activation barrier on the triplet surface is that the transition state involves the unstable d^9s^1 configuration of the Cu(I) atom. On the other hand, we cannot locate any radical intermediate on the singlet potential energy surface because of the low-lying transition state, which suggests that the product complex is formed in a barrierless fashion after the hydrogen-atom abstraction on the singlet potential energy surface. We scanned the singlet potential energy surface of the rebound step along the C–O coordinate (points 2–7), as listed in Table 5. The release of the constraint of the C–O bond distance at point 7 leads to the product complex at point 8. These results demonstrate that

(49) (a) Groves, J. T.; Haushalter, R. C.; Nakamura, M.; Nemo, T. E.; Evans, B. J. *J. Am. Chem. Soc.* **1981**, *103*, 2884. (b) Groves, J. T. *J. Chem. Educ.* **1985**, *62*, 928.

(50) Moore, C. E. *Atomic Energy Levels*; U. S. National Bureau of Standards: Washington, DC, 1949; Circular 467.

Table 5. Geometries and Energies of Selected Points, 1–8, along the Rebound Process by the Cu(III)–Oxo Species in the Singlet State

	point							
	1 ^b	2	3	4	5	6	7	8
C–O	3.010	2.900 ^a	2.800 ^a	2.700 ^a	2.600 ^a	2.500 ^a	2.450 ^a	1.462
Cu–O	1.804	1.848	1.858	1.871	1.885	1.902	1.910	3.148
energy	–14.2	–17.6	–18.6	–19.5	–20.3	–21.3	–21.7	–60.6

^a The C–O distance is constrained during a geometry optimization. All distances and energies are in angstroms and kilocalories per mole, respectively. Points 1 and 8 are fully optimized structures. ^b Values for the triplet state on the assumption of spin crossover to the singlet surface.

there is no substantial barrier for the rebound step on the singlet potential energy surface. Similar trends were found in the rebound step of alkane hydroxylation by compound I (an iron–oxo species) of P450.^{51,52} In the triplet state of the QM/MM-optimized structure of **I–oxo**, the distance between the oxygen atom of the hydroxo ligand and the carbon radical center is 3.010 Å. This is a typical value in the initial distance for the rebound process. For example, the C–O distance in the radical intermediate for camphor hydroxylation by compound I of P450 is 3.187 and 3.304 Å in the quartet and doublet states, respectively.⁵² On the other hand, the oxygen atom of the hydroxo ligand is far from the carbon radical center in the small-cluster model, the distance being 4.557 and 4.567 Å in the singlet and triplet states, respectively. The carbon radical center of the substrate radical easily moves apart from the OH ligand to form a relatively strong bond between the OH ligand and a hydrogen atom of the α -carbon in the small-cluster model; the bond distance is 2.662 and 2.655 Å in the triplet and doublet states, respectively. This new hydrogen bond overrides the weak interaction between the OH ligand and the carbon radical center that triggers the barrierless recombination. These results indicate that the surrounding amino acid residues (Glu369, Glu268, and Tyr494) play an essential role not only in the hydrogen-atom abstraction but also in the rebound process. Thus, we expect that a spin inversion can take place when the radical intermediate goes down the slope of the barrierless potential energy surface in the protein environment. The overall reaction is 60.6 kcal/mol exothermic with the spin inversion from the triplet state to the singlet state.

4. Conclusions

We have studied the mechanisms of dopamine hydroxylation by the Cu(II)–superoxo species and the Cu(III)–oxo species of dopamine β -monooxygenase (DBM) using QM/MM calculations. The whole-enzyme model of DBM constructed from the crystal structure of peptidylglycine α -hydroxylating monooxygenase (PHM) gave us detailed information on the structure of the catalytic core that is relevant

to the stereospecific hydroxylation of dopamine. The side chain of three amino acid residues (His415, His417, and Met490) coordinates to the Cu_B atom as ligands. The hydrogen-bonding network between dopamine and three amino acid residues (Glu268, Glu369, and Tyr494) plays an essential role in substrate binding and the stereospecific hydroxylation of dopamine to norepinephrine. The activation barrier for the hydrogen-atom abstraction by the Cu(II)–superoxo species is 23.1 kcal/mol, while that of the Cu(III)–oxo species is only 5.4 kcal/mol. The relative energies of the optimized radical intermediates in the superoxo- and oxo-mediated pathways are 18.4 and –14.2 kcal/mol relative to the corresponding reactant complexes, respectively. These results tell us that the Cu(III)–oxo species has a higher oxidizing power in the protein environment of DBM. The QM/MM optimized structure of the radical intermediate in the oxo-mediated pathway shows the key amino acid residues to fix the substrate radical in a proper position for the subsequent recombination process at a distance of 3.010 Å between the oxygen atom of the hydroxo ligand and the carbon radical center in the triplet state. A high activation energy is required for the recombination of dopamine radical on the triplet potential energy surface, whereas the radical intermediate barrierlessly collapses into the product complex on the singlet potential energy surface. Thus, the reaction pathway should involve a spin-inversion electronic process near the radical intermediate between the triplet and singlet potential energy surfaces. The stereospecific dopamine hydroxylation by the Cu(III)–oxo species is a downhill and lower-barrier process toward the product direction with the aid of the protein environment of DBM. We therefore conclude that this enzyme is likely to use the high reactivity of the Cu(III)–oxo species to activate the benzylic C–H bond of dopamine; the enzymatic reaction is an example of the oxygen rebound mechanism.

Acknowledgment. K.Y. acknowledges the Nanotechnology Support Project of the Ministry of Culture, Sports, Science and Technology of Japan (MEXT), the Joint Project of Materials Synthesis of MEXT, and CREST of Japan Science and Technology Cooperation for their support of this work.

IC0521168

- (51) Kamachi, T.; Yoshizawa, K. *J. Am. Chem. Soc.* **2003**, *125*, 4652.
 (52) (a) Harris, N.; Cohen, S.; Filatov, M.; Ogliaro, F.; Shaik, S. *Angew. Chem., Int. Ed.* **2000**, *39*, 2003. (b) Ogliaro, F.; Harris, N.; Cohen, S.; Filatov, M.; de Visser, S. P.; Shaik, S. *J. Am. Chem. Soc.* **2000**, *122*, 8977.